NUMERICAL ANALYSIS OF COMBINED NATURAL CONVECTION-INTERNAL HEAT GENERATION SOURCE-SURFACE RADIATION

by

Saber HAMIMID[a,b]* and Messaoud GUELLAL[a]

[a] Laboratory for Chemical Engineering, University of Ferhat Abbas Setif-1, Setif, Algeria
[b] Faculty of Sciences and Applied Sciences, University of Bouira, Bouira, Algeria

Original scientific paper
DOI: 10.2298/TSCI140315115H

Numerical study of combined laminar natural convection and surface radiation with internal heat generation is presented in this paper and computations are performed for an air-filled square cavity whose four walls have the same emissivity. Finite volume method through the concepts of staggered grid and SIMPLER algorithm has been applied, and the view factors are determined by analytical formula. A power scheme is also used in approximating advection-diffusion terms. Representative results illustrating the effects of emissivity and the internal heat generation on the streamlines and temperature contours within the enclosure are reported. In addition, obtained results for local and average convective and radiative Nusselt number, for various parametric conditions, show that internal heat generation modifies significantly the flow and temperature fields.

Key words: *natural convection, heat generation, surface radiation, numerical simulation*

Introduction

Due to its many engineering applications and impact on both flow structure and heat transfer processes in double pane windows, solar collectors, building insulation, nuclear engineering, ovens, and rooms, combined natural convection and radiation exchange between surfaces involving a radiatively non-participating medium inside enclosures has been a very important research topic. During the last decades, significant attention was given to the study of natural convection in enclosures subjected to volumetric internal heat generation, ranging from the mantle convection in the earth [1] to the cooling of a molten nuclear reactor core [2, 3]. Although the surface radiation is inherent in natural convection, the interaction between the two phenomena has received a little attention.

Many studies on laminar and turbulent natural convection heat transfer in a rectangular enclosure are carried out including radiation [4-9]. In their investigation, Lauriat and Desrayaud [10] studied numerically the heat transfer by natural convection and surface radiation in a 2-D vented enclosure in contact with a cold external environment and a hot internal one. They found that the radiative contributions to the heat transfer along the facing surfaces were the dominant heat transfer mode for all of the considered cases.

Amraqui *et al.* [11] analysed computation of the radiation-natural convection interactions in an inclined T form cavity. They conclude that the heat transfer decreases with in-

* Corresponding author; e-mail: sa_hamimid@yahoo.fr

creasing φ (inclination angle). Moreover, they noted that the Rayleigh number and the presence of radiation produce a considerable increase of the heat transfer. Nouanegue *et al.* [12] investigated conjugate heat transfer by natural convection, conduction, and radiation in open cavities in which a uniform heat flux is applied to the inside surface of the solid wall facing the opening. They noticed that the surface radiation affected the flow and temperature fields considerably. Effect of radiation on natural convection flow around a sphere in presence of heat generation was investigated by Miraj *et al.* [13]. They found that the increase in the values of radiation parameter or in surface temperature parameter, leads to increase in the velocity profile, the temperature profile, the local skin friction coefficient, and the local rate of heat transfer. The effect of radiative transfer and the aspect ratio on the 3-D natural convection has been studied by Kolsi *et al.* [14]. They showed that the principal flow structure is considerably modified when the radiation-conduction parameter was varied. However, the peripheral spiraling motion is qualitatively insensitive to these parameters. Rahman and Sharif [15] studied the laminar natural convection in differentially heated inclined rectangular enclosures of aspect ratios from 0.25 to 4. They considered a rectangular cavity with and without internal heat generation showing that the uniform internal heat generation increases the local heat flux ratio along the hot wall and decreases it along the cold wall. Recently, Pal and Mondal [16] have investigated the combined convection flow of an optically dense viscous incompressible fluid over a vertical surface embedded in a fluid saturated porous medium of variable porosity in the presence of thermal radiation and heat generation/absorption effects. Elbashbeshy *et al.* [17] studied the effect of heat generation or absorption and thermal radiation on free convection flow and heat transfer over a truncated cone in the presence of pressure work. They concluded that an increasing in the values of radiation parameter and heat generation/absorption parameter leads to increases in the value of the skin fiction coefficient while the local Nusselt number decreases. Ashraf *et al.* [18] investigated the effect of radiation on fluctuating hydromagnetic natural convection flow of viscous, incompressible, electrically conducting fluid past a magnetized vertical plate.

The studies carried out by Hamimid *et al.* [19, 20] first in the case of pure natural convection, and then in the case of combined natural convection-surface radiation showed that the Boussinesq approximation is not sufficient to simulate natural convective flow for large temperature differences, and a low Mach number flow model is more suitable under non-Boussinesq conditions. It has also been noticed that surface radiation alters significantly the heat transfer.

The purpose if this paper is to study the combined effects of surface radiation and heat generation on the flow and heat transfer in the cavity. The surface emissivity, ε_i, and the internal Rayleigh number, Ra_I, are parameters to be varied.

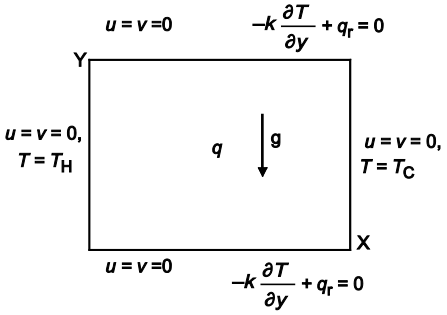

Figure 1. The flow configuration and co-ordinate system

Mathematical formulation

Details of the geometry are shown in fig. 1. The flow is assumed to be incompressible, laminar, and 2-D in an enclosure of square cavity with internal heat generation, q, the two vertical walls are maintained at two different temperatures T_H and T_C ($T_H > T_C$), while the two horizontal walls are submitted to a radiative heat flux $q_r = k\partial T/\partial y$. It will be further assumed that the temperature differences in

the domain under consideration are small enough to justify the employment of the Boussinesq approximation.

The fluid is the air and its properties are assumed constant at the average temperature, T_0, except for the density whose variation with the temperature is allowed in the buoyancy term. The inner surfaces, in contact with the fluid, are assumed to be gray and diffuse, and could emit and reflect radiation with identical emissivities.

The fluid flow state is given by the velocity vector, $\vec{V}$, the density, ρ, the pressure, P, and the temperature, T. The balance equations describing the motion of a fluid in a region of space form a set of three conservation laws:

– the equation of continuity expresses the mass conservation of the fluid particle,
– the equation of linear momentum reflects the fundamental principle of dynamics applied to the fluid particles. It states that the total change of momentum in a given volume control is equal to the sum of the forces acting in this volume and surface forces acting on its surface, and
– the energy equation requires that the energy can not be created or destroyed. It expresses the conservation of the energy of the fluid particle.

Taking into account the previously mentioned assumptions , the governing equations for the problem in two dimensions unsteady states can be written in dimensional form:

$$\frac{\partial u}{\partial x}+\frac{\partial v}{\partial y}=0 \tag{1}$$

$$\rho\left(\frac{\partial u}{\partial t}+u\frac{\partial u}{\partial x}+v\frac{\partial u}{\partial y}\right)=-\frac{\partial p}{\partial x}+\mu\left(\frac{\partial^2 u}{\partial x^2}+\frac{\partial^2 u}{\partial y^2}\right) \tag{2}$$

$$\rho\left(\frac{\partial v}{\partial t}+u\frac{\partial v}{\partial x}+v\frac{\partial u}{\partial y}\right)=-\frac{\partial p}{\partial y}+\mu\left(\frac{\partial^2 v}{\partial x^2}+\frac{\partial^2 v}{\partial y^2}\right)+\rho g\beta(T-T_0) \tag{3}$$

$$\frac{\partial T}{\partial t}+u\frac{\partial T}{\partial x}+v\frac{\partial T}{\partial y}=\alpha\left(\frac{\partial^2 T}{\partial x^2}+\frac{\partial^2 T}{\partial y^2}\right)+\frac{q}{\rho c_p} \tag{4}$$

Introducing the following non-dimensional variables:

$$X=\frac{x}{H},\quad Y=\frac{y}{H},\quad U=\frac{uH}{\alpha},\quad V=\frac{vH}{\alpha},\quad P=\frac{pH^2}{\rho\alpha^2},\quad \theta=\frac{T-T_0}{\Delta T},\quad \tau=\frac{t}{\frac{H^2}{\alpha}},\quad \Delta T=T_{\mathrm{H}}-T_{\mathrm{C}}$$

Dimensionless governing eqs. (1)-(4) can be written:

$$\frac{\partial U}{\partial X}+\frac{\partial V}{\partial Y}=0 \tag{5}$$

$$\frac{\partial U}{\partial \tau}+U\frac{\partial U}{\partial X}+V\frac{\partial U}{\partial Y}=-\frac{\partial P}{\partial X}+\mathrm{Pr}\left(\frac{\partial^2 U}{\partial X^2}+\frac{\partial^2 U}{\partial Y^2}\right) \tag{6}$$

$$\frac{\partial V}{\partial \tau}+U\frac{\partial V}{\partial X}+V\frac{\partial V}{\partial Y}=-\frac{\partial P}{\partial Y}+\mathrm{Pr}\left(\frac{\partial^2 V}{\partial X^2}+\frac{\partial^2 V}{\partial Y^2}\right)+\mathrm{Ra}_{\mathrm{E}}\,\mathrm{Pr}\,\theta \tag{7}$$

$$\frac{\partial\theta}{\partial\tau}+U\frac{\partial\theta}{\partial X}+V\frac{\partial\theta}{\partial Y}=\left(\frac{\partial^2\theta}{\partial X^2}+\frac{\partial^2\theta}{\partial Y^2}\right)+\frac{\mathrm{Ra_I}}{\mathrm{Ra_E}} \tag{8}$$

where $\mathrm{Ra_E}$ and $\mathrm{Ra_I}$ are the external and the internal Rayleigh numbers defined, respectively:

$$\mathrm{Ra_E}=\frac{\mathrm{g}\beta\Delta TH^3}{\nu\alpha},\qquad \mathrm{Ra_I}=\frac{\mathrm{g}\beta qH^5}{\nu\alpha k}$$

The corresponding initial and boundary conditions are:

$$U=V=0,\quad \theta=\theta_i\quad \text{for}\quad \tau=0$$

$$U=V=0,\quad \theta=\theta_\mathrm{C}=-0.5\quad \text{for}\quad 0\le Y\le 1\quad \text{at}\quad X=0$$

$$U=V=0,\quad \theta=\theta_\mathrm{H}=0.5\quad \text{for}\quad 0\le Y\le 1\quad \text{at}\quad X=1$$

$$U=V=0,\quad \partial\theta/\partial Y-NrQ_\mathrm{r}=0\quad \text{for}\quad 0\le X\le 1\quad \text{at}\quad Y=0$$

$$U=V=0,\quad \partial\theta/\partial Y-NrQ_\mathrm{r}=0\quad \text{for}\quad 0\le X\le 1\quad \text{at}\quad Y=1$$

where $Nr=\sigma T_0^4H/k\Delta T$, is the dimensionless parameter of conduction-radiation and $Q_\mathrm{r}=q_\mathrm{r}/\sigma T_0^4$ – the dimensionless net radiative heat flux.

Therefore, the dimensionless net radiative flux density along a diffuse-gray and opaque surface A_i is expressed:

$$Q_{\mathrm{r},i}=R_i-\sum_{j=1}^{N}R_jF_{i-j} \tag{9}$$

where R_i is the dimensionless radiosity of surface A_i, obtained by resolving the system:

$$\sum_{j=1}^{N}[\delta_{ij}-(1-\varepsilon_i)F_{i-j}]R_j=\varepsilon_i\Theta_i^4 \tag{10}$$

where the dimensionless radiative-temperature Θ_i is given by:

$$\Theta_i=\frac{T_i}{T_0}=\frac{(T_\mathrm{H}-T_\mathrm{C})\theta_i+T_0}{T_0}=\theta_i\frac{\Delta T}{T_0}+1 \tag{11}$$

$$\Theta_i=\frac{\theta_i}{\theta_0}+1 \tag{12}$$

Numerical procedure

The numerical solution of the governing differential equations for the velocity, pressure, and temperature fields is obtained by using a finite volume technique. A power scheme was also used in approximating advection-diffusion terms. The SIMPLER algorithm whose details can be found in Patankar [21], with a staggered grid is employed to solve the coupling between pressure and velocity. The governing equations are cast in transient form and a fully implicit transient differencing scheme was employed as an iterative procedure to reach steady-state. The discretised equations are solved using the line by line Thomas algorithm with two directional sweeps.

The radiosities of the elemental wall surfaces are expressed as a function of elemental wall surface temperature, emissivity, and the shape factors. The radiosity, R_i, and temperature, Θ_i, are connected by eq. (10) whose resolution is performed by the Gauss elimination method. In 2-D, the view factors are analytic [22]:

$$F_{i-j} = \frac{-1}{2(x_2 - x_1)}\left(\sqrt{x_2^2 + y^2}\Big|_{y_1}^{y_2} - \sqrt{x_1^2 + y^2}\Big|_{y_1}^{y_2} \right) \tag{13}$$

$$F_{i-k} = -\frac{1}{2(x_2 - x_1)}\left[\sqrt{(\underline{x}_2 - x)^2 + H^2}\Big|_{x=x_1}^{x=x_2} - \sqrt{(\underline{x}_1 - x)^2 + H^2}\Big|_{x=x_1}^{x=x_2} \right] \tag{14}$$

For the calculations reported in this study, a 120 × 120 grid points was chosen to optimise the relation between the accuracy required and the computing time. In order to obtain good convergence solutions, the convergence criterion for the residuals was set at 10^{-5}.

The outer iterative loop is repeated until the steady-state is achieved which occurs when the following convergences are simultaneously satisfied: $|\phi_{ij}^{\text{old}} - \phi_{ij}| \le \varepsilon_\phi$, where ϕ represents the variables U, V, or θ. In most of the cases, the velocity components and temperatures were driven to $\varepsilon_U = \varepsilon_V = \varepsilon_\theta \le 10^{-6}$.

Validation

In order to verify the numerical code, the model is reduced to the classical case of natural convection and surface radiation in a square cavity without heat generation. The convective, radiative, and total Nusselt numbers of the active walls are compared with the ones of Wang [23]. The results presented in tab. 1 show an excellent agreement.

Table 1. Nusselt numbers at vertical walls with T_0 = 293.5 K, and ΔT = 10 K

Ra_E	H	ε	Ref. [23]						Present study					
			Hot wall			Cold wall			Hot wall			Cold wall		
			Nu_c	Nu_r	Nu_t	Nu_c	Nu_r	Nu_t	Nu_c	Nu_r	Nu_t	Nu_c	Nu_r	Nu_t
10^4	0.021	0	2.246	0	2.246	2.246	0	2.246	2.246	0	2.246	2.246	0	2.246
10^4	0.021	0.2	2.260	0.507	2.767	2.268	0.499	2.767	2.262	0.507	2.769	2.271	0.498	2.769
10^4	0.021	0.8	2.249	2.401	4.650	2.278	2.372	4.650	2.255	2.401	4.656	2.284	2.371	4.656
10^5	0.045	0	4.540	0	4.540	4.540	0	4.540	4.532	0	4.532	4.532	0	4.532
10^5	0.045	0.2	4.394	1.090	5.484	4.411	1.073	5.484	4.398	1.090	5.489	4.417	1.072	5.489
10^5	0.045	0.8	4.189	5.196	9.385	4.247	5.137	9.384	4.200	5.196	9.397	4.261	5.136	9.397
10^6	0.097	0	8.852	0	8.852	8.852	0	8.852	8.863	0	8.863	8.863	0	8.863
10^6	0.097	0.2	8.381	2.355	10.736	8.417	2.319	10.736	8.379	2.355	10.734	8.416	2.318	10.734
10^6	0.097	0.8	7.815	11.265	19.080	7.930	11.150	19.078	7.861	11.265	19.126	7.971	11.151	19.126

Results and discussions

This section is devoted to analyse the effects of the internal heat generation parameter, Ra_I, on the flow and heat transfer on the combined natural convection surface radiation flow considering Pr = 0.70, T_0 = 300 K, $Ra_E = 10^6$, ΔT = 10 K, and ε = (0.2, 0.5).

For low internal Rayleigh number Ra_I ($\le 10^7$), considerations are given to the cases when the effects of external heating and internal heat generation are comparable. Figures 2 and 3 illustrate the sequences of flow and thermal fields for ε = 0.2 and ε = 0.5, respectively. Performing order of magnitude analysis on Ra_I = 0, and 10^6, implies that the relative impact of internal heat generation is minor. The flow is attributed by the presence of a single clock-

wise circulation cell, which occupies much of the cavity and a secondary and a tertiary vortices are formed inside the cavity (vortices of surface radiation effects without internal heat generation, $Ra_I = 0$).

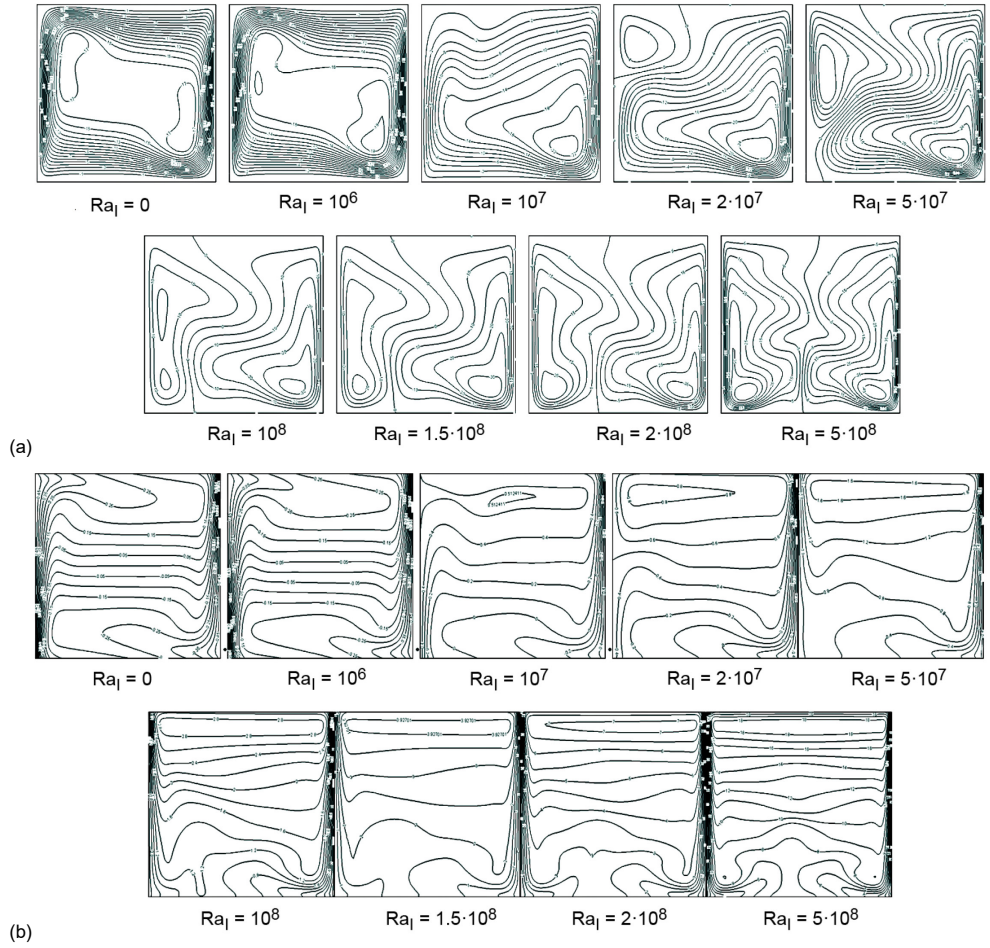

Figure 2. (a) Streamlines, (b) Isotherms for $\varepsilon = 0.2$, and various values of Ra_I

As the heat generation increases, ($Ra_I \geq 10^7$), the total thermal energy in the cavity is on increase, those small vortices are merged to the primary vortex of relatively higher intensity of circulation than that at low Ra_I.

Consequently, a counter-clockwise small cell appeared at the upper left corner (for $Ra_I = 2 \cdot 10^7$), and is shifted left with increasing Ra_I. The flow strength in this new cell also increases when the internal heat generation increases in magnitude.

For large values of internal Rayleigh number, the whole cavity is occupied by two recirculating cells; *i. e.* both counter-clockwise and clockwise cells near the hot and cold side walls, respectively, due to the positive buoyancy effect. The isotherms tend to be horizontally uniform and vertically linear at the upper portion of the enclosure. However, in the bottom part of the cavity, the isotherms are divided into two groups.

This effect of internal heat generation on the flow field is reasonable since internal heat generation assists buoyancy forces by accelerating the fluid flow, figs .4(a)-(c).

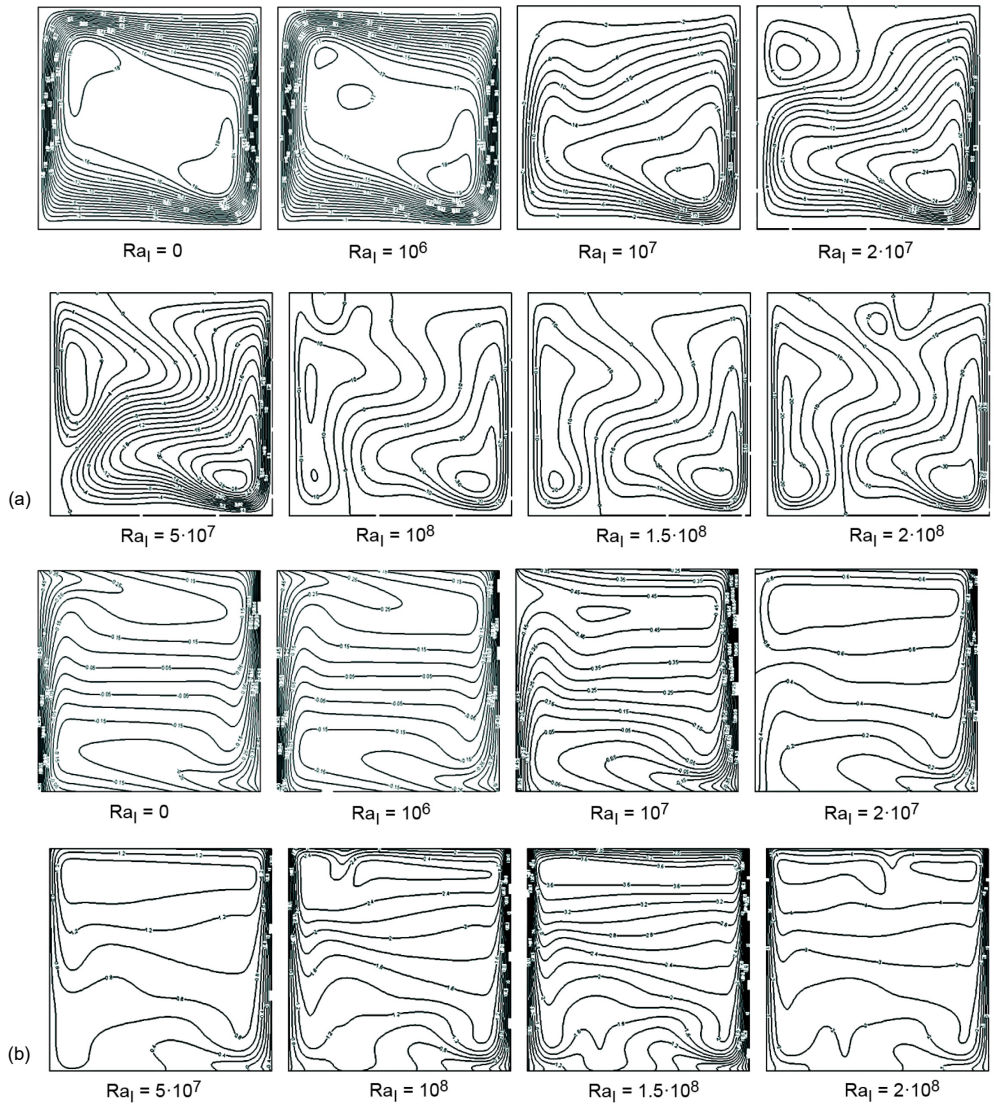

Figure 3. (a) Streamlines, (b) Isotherms for ε = 0.5 and various values of Ra$_I$

On the other hand, the presence of heat source within the enclosure causes an increase in the fluid temperature, fig. 4(d), leading to a reduction of convective and radiative heat transfer on the hot wall, figs. 5 and 6.

From fig. 5, we can also note that for weak heat generation, local convective Nusselt number has positive values at the upper section of the cavity, and from $Ra_I = 2\cdot10^7$ all values are negative. This means that, the heat is transferred from the fluid to the hot wall (the hot wall absorbs the heat from the interior higher temperature fluid). The same behaviour is observed for the local radiative Nusselt number at $Ra_I = 5\cdot10^7$ (fig. 6).

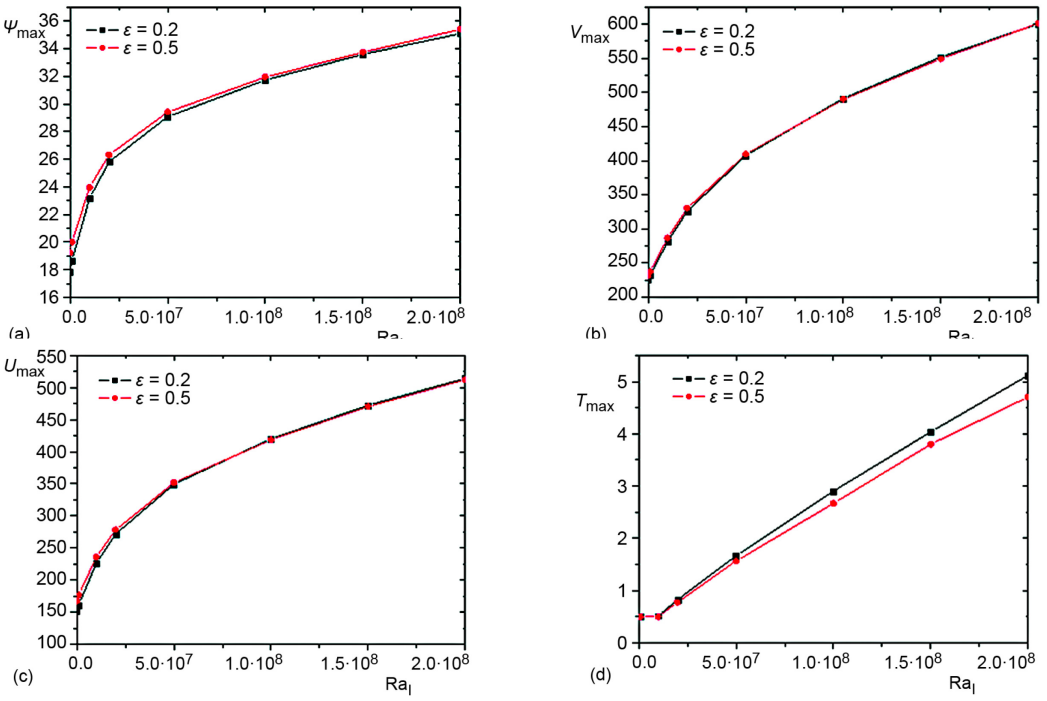

Figure 4. Variations of (a) maximum values of the stream function, (b) vertical velocity, (c) horizontal velocity, and (d) temperature with internal Rayleigh number for $Ra_E = 10^6$

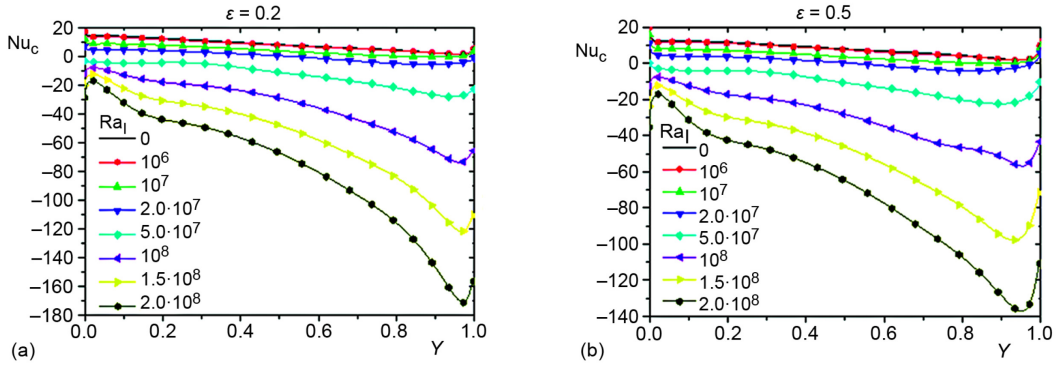

Figure 5. Local convection Nusselt number on the hot wall for $Ra_E = 10^6$

The negative sign of Nu_c and Nu_r corresponds to the apparition of the small counter-clockwise cell shown previously in fig. 2. It is noticeable that the absolute value for the temperature gradient has a maximum value at this position, since this cell is coming to the hot wall at the upper corner. Therefore, the values of Nu_c and Nu_r along the hot side wall are governed by the direction and strength of the flow adjacent to the hot wall.

Figure 7 illustrates the variation of average convective and radiative Nusselt numbers for different values of internal heat generation and emissivity. The positive values of

$Nu_{c,\,avg}$ and $Nu_{r,\,avg}$ mark that there is ascending motion near the hot wall though the circulation feels retardation due to the buoyancy effect generated by internal heat generation. Therefore, as Ra_I increases, the average convective and radiative Nusselt numbers decrease indicating the descending motion near the hot side wall.

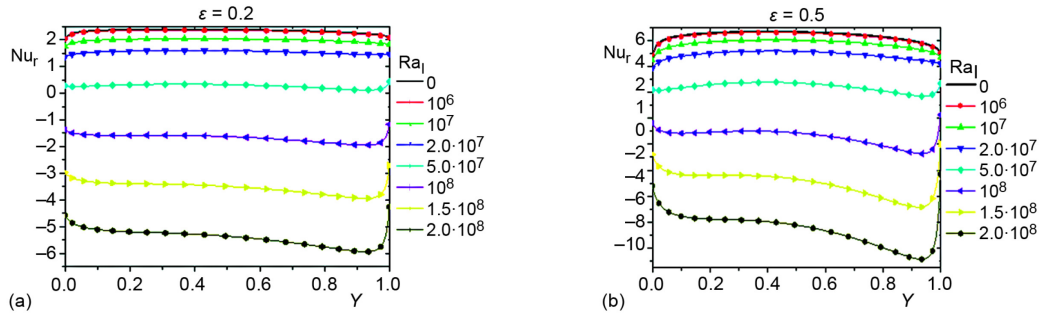

Figure 6. Local radiation Nusselt number on the hot wall for $Ra_E = 10^6$

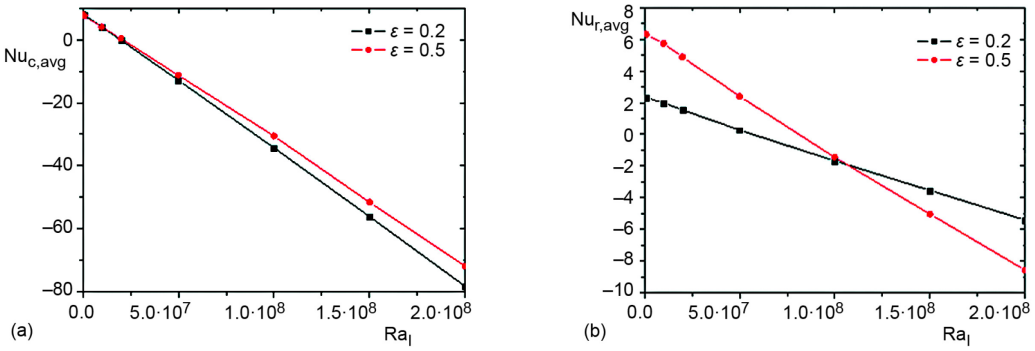

Figure 7. Variations of the average (a) convection and (b) radiation Nusselt number as a function of internal Rayleigh number

Conclusion

In the present numerical investigation, calculations have been made for the combined natural convection and surface radiation in a differentially cavity with the presence of an internal heat generation. The study shows that internal heat generation modifies significantly the flow and temperature fields. The increase in the value of the heat generation parameter leads to increase in the flow rates in the secondary cell as well an increase in its size until it occupies the half of the total cavity space. Further increase in the value of heat generation causes for development of more cells in the cavity. The temperature of the fluid in the cavity also increases due to the increase of internal heat generation and hence that negates the heat transfer from the heated surface.

Nomenclature

A_i – radiative surface number of i
c_p – specific heat at constant pressure, [$Jkg^{-1}K^{-1}$]
F_{i-j} – view factor between surfaces S_i and S_j
g – gravitational acceleration, [ms^{-2}]
H – height of the enclosure, [m]
k – thermal conductivity, [$Wm^{-1}K^{-1}$]
N – total number of radiative surfaces

Nr – radiation number, $[=\sigma T_0^4(k\Delta T/H)]$
Nu – Nusselt number
P – dimensionless pressure, [Pa]
p – fluid pressure, [Pa]
Pr – Prandtl number, $(=\nu/\alpha)$
Q_r – dimensionless net radiative-flux
q – internal heat generation [Wm^{-3}]
q_r – net radiative flux, [Wm^{-2}]
R_i – dimensionless radisosity
Ra – Rayleigh number
T – dimensional temperature, [K]
ΔT – temperature difference, $(=T_C - T_F)$, [K]
t – time, [s]
U, V – dimensionless velocity-components
u, v – dimensional velocity-components, [ms^{-1}]
X, Y – dimensionless co-ordinates
x, y – cartesian co-ordinates, [m]

Greek symbols

α – thermal diffusivity, [m^2s^{-1}]
β – thermal expansion coefficient [K^{-1}]
ε_i – emissivity of surface A_i
μ – dynamic viscosity of the fluid, [$kgm^{-1}s^{-1}$]
ν – kinematic viscosity, [m^2s^{-1}]
ρ – fluid density, [kgm^{-3}]
σ – Stefan-Boltzmann constant, [$Wm^{-1}K^{-4}$]
θ – dimensionless temperature, $(=T - T_0)/\Delta T$
Θ_i – dimensionless temperature, $(=T/T_0)$
δ_{ij} – Kronecker symbol
τ – dimensionless time

Subscripts

avg – average value
C – cold
c – convective
E – external
I – internal
H – hot
max – maximum value
r – radiative
t – total
0 – reference state

References

[1] Travis, B., *et al*., Three-Dimensional Convection Planforms with Internal Heat Generation, *Geophys. Res. Lett.*, *17* (1990), 3, pp. 243-246
[2] Sharmaa, A., *et al*., Conjugate Transient Natural Convection in a Cylindrical Enclosure with Internal Volumetric Heat Generation, *Ann. Nucl. Energ. 35* (2008), 8, pp. 1502-1514
[3] Lee, S. D., *et al*., Natural Convection Thermo Fluid Dynamics in a Volumetrically Heated Rectangular Pool, *Nucl. Eng. Des.*, *237* (2007), 5, pp. 473-483
[4] Balaji, C., Venkateshan, S. P., Combined Surface Radiation and Free Convection in Cavities, *J. Thermophys. Heat Transfer*, *8* (1994), 2, pp. 373-376
[5] Ramesh, N., Venkateshan, S. P., Effect of Surface Radiation on Natural Convection in a Square Enclosure, *J. Thermophys. Heat Transfer*, *13* (1999), 3, pp. 299-301
[6] Velusamy, K., *et al*., Interaction Effects between Surface Radiation and Turbulent Natural Convection in Square and Rectangular Enclosures, *J. Heat Transfer, 123* (2001), 6, pp. 1062-1070
[7] Anil, K. S., *et al*., Conjugate Turbulent Natural Convection with Surface Radiation in Air Filled Rectangular Enclosures, *Int. J. Heat Mass Transfer*, *50* (2007), 3, pp. 625-639
[8] Alvarado, R., *et al*., Interaction between Natural Convection and surface Thermal Radiation in Tilted Slender Cavities, *Int. J. Thermal Sciences*, *47* (2008), 4, pp. 355-368
[9] Xaman, J., *et al*., Laminar and Turbulent Natural Convection Combined with Surface Thermal Radiation in a Square Cavity with a Glass Wall, *International Journal of Thermal Sciences*, *47* (2008), 12, pp. 1630-1638
[10] Lauriat, G., Desrayaud, G., Effect of Surface Radiation on Conjugate Natural Convection in Partially Open Enclosures, *International Journal of Thermal Sciences*, *45* (2006), 4, pp. 335-346
[11] Amraqui, S., *et al*., Computation of Coupled Surface Radiation and Natural Convection in an Inclined "T" Form Cavity, *Energy Conversion and Management, 52* (2011), 12, pp. 1166-1174
[12] Nouanegue, H., *et al*., Conjugate Heat Transfer by Natural Convection, Conduction and Radiation in Open Cavities, *International Journal of Heat and Mass Transfer, 51* (2008), 25, pp. 6054-6062
[13] Miraj, M., *et al*., Effect of Radiation on Natural Convection Flow on a Sphere in Presence of Heat Generation. *International Communications in Heat and Mass Transfer, 37* (2010), 6, pp. 660-665
[14] Kolsi, L., *et al*, Combined Radiation-Natural Convection in Three-Dimensional Verticals, *Thermal Science*, *15* (2011), Suppl. 2, pp. S327-S339
[15] Rahman, R., Sharif, M. A., Numerical Study of Laminar Natural Convection in Inclined Rectangular Enclosures of Various Aspect Ratios, *Num. Heat Transfer Part A*, *44* (2003), 4, pp. 355-373

[16] Pal, D., Mondal, H., Effect of Variable Viscosity on MHD Non-Darcy Mixed Convective Heat Transfer over a Stretching Sheet Embedded in a Porous Medium with Non-Uniform Heat Source/Sink, *Communications in Nonlinear Science and Numerical Simulation*, *15* (2010), 6, pp. 1553-1564
[17] Elbashbeshy, E. M. A., *et al*., Effect of Thermal Radiation on Free Convection Flow and Heat Transfer over a Truncated Cone in the Presence of Pressure Work and Heat Generation/Absorption*, Thermal Science*, *20* (2016), 2, pp. 555-565
[18] Ashraf, M., *et al*., Fluctuating Hydromagnetic Natural Convection Flow Past a Magnetized Vertical Surface in the Presence of Thermal Radiation, *Thermal Science*, *16* (2012), 4, pp. 1081-1096
[19] Hamimid, S., *et al*., Numerical Study of Natural Convection in a Square Cavity under Non-Boussinesq Conditions, *Thermal Science*, *20* (2016), 5, pp. 1509-1517
[20] Hamimid, S., *et al.,* Numerical Simulation of Combined Natural Convection Surface Radiation for Large Temperature Gradient, *Journal of Thermophysics and Heat Transfer, 29* (2015), 3, pp. 636-646
[21] Patankar, S. V., *Numerical Heat Transfer and Fluid Flow*, McGraw-Hill, New York, USA, 1980
[22] Howell, J. R., *A Catalog of Radiation Configuration Factors*, McGraw-Hill, New York, USA, 1982
[23] Wang, H., *et al*., Numerical Study of Natural Convection-Surface Radiation Coupling in Air-Filled Square Cavities (in French), *Comptes Rendus Mecanique, 334* (2006), 1, pp. 48-57

Paper submitted: March 15, 2014
Paper revised: August 17, 2014
Paper accepted: August 17, 2014